

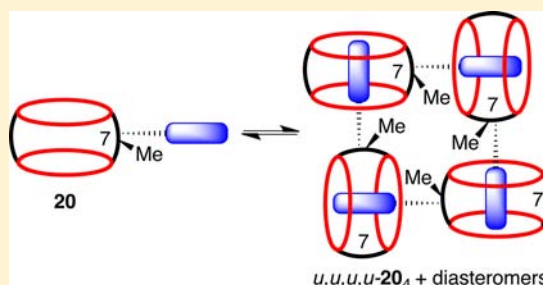
# Synthesis and Self-Assembly Processes of Monofunctionalized Cucurbit[7]uril

Brittany Vinciguerra,<sup>‡</sup> Liping Cao,<sup>‡</sup> Joe R. Cannon, Peter Y. Zavalij, Catherine Fenselau, and Lyle Isaacs\*

Department of Chemistry and Biochemistry, University of Maryland, College Park, Maryland 20742, United States

**S** Supporting Information

**ABSTRACT:** We present a building-block approach toward functionalized CB[7] derivatives by the condensation of methylene-bridged glycoluril hexamer **1** and glycoluril bis(cyclic ethers) **2** and **12**. The CB[7] derivatives Me<sub>2</sub>CB[7] and CyCB[7] are highly soluble in water (264 mM and 181 mM, respectively). As a result of the high intrinsic solubility of Me<sub>2</sub>CB[7], it is able to solubilize the insoluble benzimidazole drug albendazole. The reaction of hexamer **1** with glycoluril derivative **12**, which bears a primary alkyl chloride group, gives CB[7] derivative **18** in 16% isolated yield. Compound **18** reacts with NaN<sub>3</sub> to yield azide-substituted CB[7] **19** in 81% yield, which subsequently undergoes click reaction with propargylammonium chloride (**21**) to yield CB[7] derivative **20** in 95% yield, which bears a covalently attached triazolyl ammonium group along its equator. The results of NMR spectroscopy (<sup>1</sup>H, variable-temperature, and DOSY) and electrospray mass spectrometry establish that **20** undergoes self-assembly to form a cyclic tetrameric assembly (**20<sub>4</sub>**) in aqueous solution. CB[7] derivatives bearing reactive functional groups (e.g., N<sub>3</sub>, Cl) are now available for incorporation into more complex functional systems.

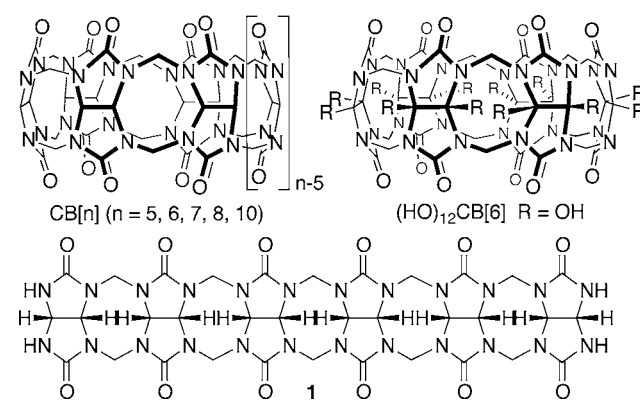


## INTRODUCTION

The cucurbit[*n*]uril (CB[*n*]; *n* = 5, 6, 7, 8, 10) family of molecular containers<sup>1,2</sup> is formed by the condensation reaction of glycoluril and formaldehyde under strongly acidic conditions.<sup>3–5</sup> The defining structural features of the CB[*n*] compounds (Chart 1) are their two symmetry-equivalent ureidyl C=O portals and their hydrophobic cavity, which imparts the ability to bind to hydrophobic and cationic species in water by a combination of ion–dipole interactions and the hydrophobic effect.<sup>6</sup> CB[*n*] compounds have emerged as a truly privileged class of receptors for molecular recognition in water as a result of their high affinity (*K<sub>a</sub>* routinely 10<sup>6</sup>–10<sup>12</sup> M<sup>-1</sup>) and their highly selective and stimuli-responsive binding processes.<sup>6–8</sup> Accordingly, CB[*n*] compounds have been used in a wide range of applications, including drug delivery,<sup>9–11</sup> molecular machines,<sup>12</sup> supramolecular polymers,<sup>13</sup> sensing ensembles,<sup>14</sup> and biomimetic systems.<sup>15</sup> Despite the wide range of applications that are enabled by CB[*n*] molecular containers, there is an ongoing need for versatile synthetic approaches toward functionalized CB[*n*] compounds that retain their recognition properties and can be incorporated into more complex functional systems. Until quite recently, the only route to functionalized CB[*n*] compounds involved the direct (per)hydroxylation of CB[*n*] introduced by Kim.<sup>16,17</sup> Kim and co-workers have used these functionalized CB[*n*] compounds in a variety of applications, including nanocapsules for drug delivery, membrane protein fishing, and hydrogels for cellular engineering.<sup>10,18,19</sup> Recently, Scherman and co-workers tamed the (per)hydroxylation reaction, which allowed them to

isolate (HO)<sub>1</sub>CB[6] and perform subsequent functionalization reactions to deliver a self-complexing CB[6] derivative.<sup>20</sup>

**Chart 1. Structure of CB[*n*], (HO)<sub>12</sub>CB[6], and Hexamer 1**



Our group has been investigating the mechanism of CB[*n*] formation<sup>21–24</sup> as a route to prepare CB[*n*]-type receptors with exciting structures and functions. For example, we have used this mechanistic knowledge to prepare CB[*n*]-type receptors that display homotropic allostery and chiral recognition, and are useful in drug delivery applications.<sup>11,25</sup> In 2011, we reported the templated synthesis of methylene-bridged glycoluril hexamer **1** and its transformation into monofunctionalized

Received: June 15, 2012

Published: July 16, 2012

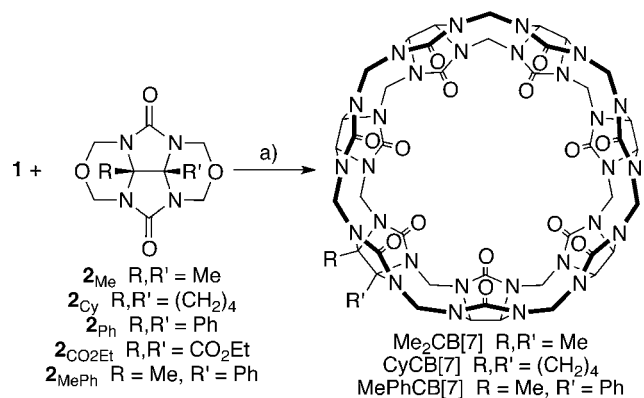
CB[6] derivatives by macrocyclization reactions with substituted phthalaldehydes.<sup>24</sup> Very recently, we reported the synthesis of a clickable CB[6] derivative, its transformation into a CB[6] derivative functionalized with an ammonium ion tail, and its self-assembly into a cyclic [c2] daisy chain assembly.<sup>26</sup> Despite the recent advances in the synthesis of monofunctionalized CB[6] derivatives,<sup>20,24,26</sup> there is still an unmet need for versatile synthetic routes toward CB[7] derivatives,<sup>16,18,27</sup> and especially monofunctionalized CB[7] derivatives that are amenable to further functionalization reactions. For example, CB[7] is nicely soluble in water, whereas CB[6] and the CB[6] derivatives prepared by us possess only modest solubility in the absence of guest. In addition, the more spacious cavity of CB[7] and its derivatives are able to bind to a wider variety of chemically and biologically interesting guests. Finally, the  $K_a$  values achieved with CB[7] are unsurpassed. In this paper we present a building-block approach<sup>21,22,27–30</sup> toward monofunctionalized CB[7] derivatives and report on their self-assembly behavior.

## RESULTS AND DISCUSSION

This section is organized as follows. First, we discuss the preparation of CB[7] derivatives Me<sub>2</sub>CB[7], CyCB[7], and MePhCB[7] by a building-block approach using glycoluril hexamer **1** and glycoluril bis(cyclic ethers) **2**. Then, we describe their basic properties (e.g., X-ray crystallography, host–guest binding, aqueous solubility, and drug solubilization). Next, we synthesize monofunctionalized CB[7] derivatives that contain reactive alkyl chloride and azide functional groups. Finally, we describe the self-assembly of a CB[7] derivative to yield a cyclic tetrameric assembly in water.

**Synthesis of Me<sub>2</sub>CB[7] and CyCB[7].** Given the ready access to gram scale quantities of glycoluril hexamer **1** and glycoluril bis(cyclic ethers) **2**, we decided to investigate their transformation into CB[7] derivatives (Scheme 1). After some

**Scheme 1.** Synthesis of Me<sub>2</sub>CB[7], CyCB[7], and MePhCB[7]<sup>a</sup>



<sup>a</sup>Conditions: (a) 9 M H<sub>2</sub>SO<sub>4</sub>, 110 °C, KI, 30 min.

experimentation, we performed the reaction between **1** and **2**<sub>Me</sub> with added KI in 9 M H<sub>2</sub>SO<sub>4</sub> at 110 °C for 30 min.<sup>31</sup> Analysis of the crude reaction mixture using *p*-xylenediammonium ion (**3**) as <sup>1</sup>H NMR probe<sup>24</sup> showed the presence of a 55:45 ratio of CB[6] and Me<sub>2</sub>CB[7]. As expected, the major competing reaction in this hexamer plus monomer building-block approach to CB[7] derivatives is the unimolecular cyclization of hexamer to give CB[6]. Purification of the mixture was

achieved by the addition of aqueous KI to an aqueous solution of the crude reaction mixture, which results in precipitation of most of the CB[6] byproduct, followed by final purification by treatment with activated carbon to yield Me<sub>2</sub>CB[7] (380 mg) in 31% yield. A similar reaction was performed between **1** and **2**<sub>Cy</sub>, which delivered CyCB[7] in 18% yield. We find that Me<sub>2</sub>CB[7] (≥264 mM) and CyCB[7] (≥181 mM) are significantly more soluble in water than CB[7] itself (20–30 mM),<sup>1</sup> which suggests that they might find utility in applications where highly soluble compounds are needed (e.g., supramolecular polymers or drug solubilization).<sup>32</sup> When we performed related reactions with **2**<sub>Ph</sub> or **2**<sub>CO<sub>2</sub>Et</sub>, we did not observe the formation of any CB[7] derivatives but rather observed the formation of CB[6] by unimolecular cyclization of **1**. From our previous work<sup>21,33</sup> we know that **2**<sub>Ph</sub> and **2**<sub>CO<sub>2</sub>Et</sub> are less reactive than alkylated glycolurils **2**<sub>Me</sub> and **2**<sub>Cy</sub>, which makes them less able to undergo bimolecular reaction with **1** to give CB[7] derivatives. In contrast, however, a similar reaction between **1** and **2**<sub>MePh</sub> resulted in a mixture of CB[6] and MePhCB[7] in a 61:30 ratio based on <sup>1</sup>H NMR analysis of the crude reaction mixture in the presence of **3**. Pure MePhCB[7] could only be obtained in a meager 3% yield after Dowex ion-exchange chromatography.

**X-ray Crystal Structure of Me<sub>2</sub>CB[7].** We were fortunate to obtain single crystals of Me<sub>2</sub>CB[7] as its Me<sub>2</sub>CB[7]·3 complex and to solve its structure by X-ray crystallography. Figure 1a shows a cross-eyed stereoview of the structure of one

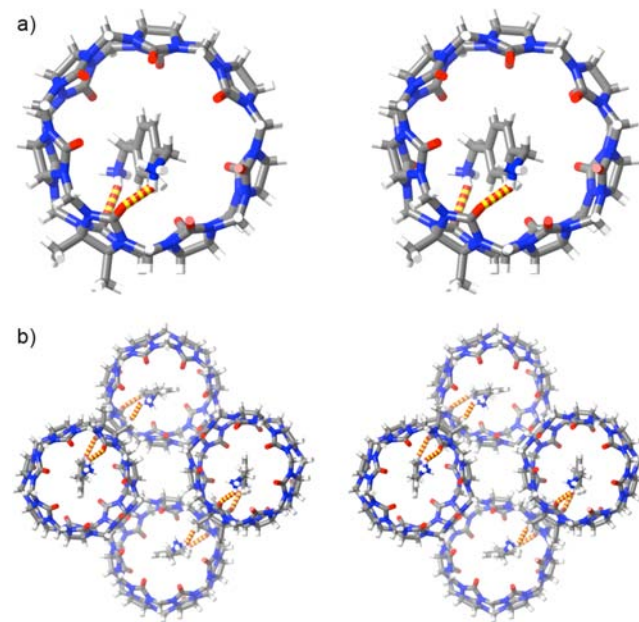


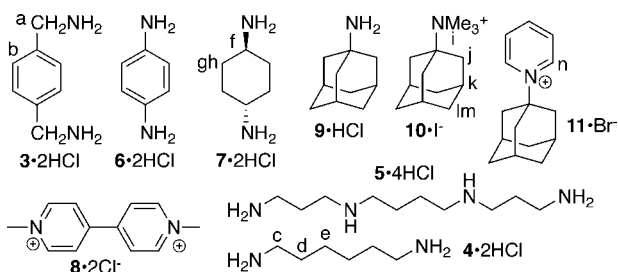
**Figure 1.** Cross-eyed stereoviews of (a) the X-ray crystal structure of Me<sub>2</sub>CB[7]·3 and (b) a portion of the crystal lattice showing the three-dimensional packing motif. Color code: C, gray; H, white; N, blue; O, red; H-bonds, red-yellow striped.

of the Me<sub>2</sub>CB[7]·3 complexes in the crystal. In contrast to CB[6] derivatives, which display an ellipsoidal deformation along their equator upon functionalization,<sup>24,29</sup> the CB[7] derivative Me<sub>2</sub>CB[7] appears structurally similar to CB[7] itself.<sup>4</sup> For example, the distance between the ureidyl C=O O-atoms of a single glycoluril unit averages 6.05 Å (range 5.87–6.154 Å), which is comparable to that observed for CB[7] (6.05 Å; range 5.913–6.114 Å) itself. Similarly, the dimensions along

the equator of Me<sub>2</sub>CB[7] are comparable to those of CB[7]. For example, the distance between the opposing methine C-atoms on each fourth glycoluril on Me<sub>2</sub>CB[7] averages 11.398 Å (range 11.247–11.516 Å), whereas for CB[7] it averages 11.404 Å (range 11.173–11.591 Å). One structural parameter that is rather different for CB[7] and Me<sub>2</sub>CB[7] is the average distance between ureidyl C=O O-atoms on every fourth glycoluril at one portal. For Me<sub>2</sub>CB[7] the distances average 8.188 Å (range 7.197–9.026 Å; standard deviation = 0.644 Å), whereas for CB[7] the distances average 8.139 Å (range 7.553–8.718 Å, standard deviation = 0.364 Å). The glycolurils appear to pivot such that one O-atom moves inward and one moves outward, which results in the ureidyl C=O portals undergoing an ellipsoidal deformation. Overall, the molecular structures of the cavity of CB[7] and Me<sub>2</sub>CB[7] are similar. Figure 1b shows a cross-eyed stereoview of the basic packing of individual complexes of Me<sub>2</sub>CB[7]·3 into a square array parallel to the *xy*-plane within the crystal. The Me groups of two adjacent Me<sub>2</sub>CB[7]·3 complexes orient themselves toward each other's ureidyl C=O portals. The iodide counterions (not depicted) are found at the corners of the square array and extend in columns along the *z*-axis.

**Molecular Recognition Properties of Me<sub>2</sub>CB[7] and CyCB[7].** After establishing the basic structural features of Me<sub>2</sub>CB[7], we decided to investigate its molecular recognition properties. For this purpose, we used guests 3–11, shown in Chart 2, which increase in size from hexanediamine 4 to

#### Chart 2. Structure of Guests Used in This Study



adamantane derivatives 9–11. Guests 3–11 are well known to form complexes with unsubstituted CB[7] with binding constants up to  $4.2 \times 10^{12} \text{ M}^{-1}$  for CB[7]·9.<sup>7</sup> Figure 2 shows the <sup>1</sup>H NMR spectra recorded for Me<sub>2</sub>CB[7]·3, Me<sub>2</sub>CB[7]·4, Me<sub>2</sub>CB[7]·7, and Me<sub>2</sub>CB[7]·10. The guest resonances observed in <sup>1</sup>H NMR spectra are nearly identical in chemical shift to those measured for the corresponding CB[7] complexes (Supporting Information), which indicates that the magnetic environments inside the cavities of CB[7] and Me<sub>2</sub>CB[7] are quite similar. The resonances observed in the <sup>1</sup>H NMR spectra that correspond to the H-atoms of C<sub>2v</sub>-symmetric Me<sub>2</sub>CB[7] reflect its lower symmetry. For example, three doublets of relative integral 2, and one doublet of relative integral 1, are observed for the upfield-shifted H-atoms of the diastereotopic CH<sub>2</sub> groups of the Me<sub>2</sub>CB[7]·3 complex (Figure 2a). The main reason for synthesizing CB[7] derivatives is to be able to incorporate them into more complex systems while maintaining their recognition properties. Therefore, we viewed it as critical to verify that the high binding constants observed for CB[7] are maintained for CB[7] derivatives like Me<sub>2</sub>CB[7]. For this purpose, we used the complexes CB[7]·11 and Me<sub>2</sub>CB[7]·11, because the H-atoms adjacent to the pyridinium N-atom are located at the ureidyl C=O portal in the

complexes. Given that the presence of the two Me groups induces a change in the O...O distance in the substituted glycoluril (*vide supra*), we thought that these protons might exhibit different chemical shifts in the CB[7]·11 and Me<sub>2</sub>CB[7]·11 complexes. Experimentally, we find that H<sub>n</sub> resonates at 8.95 ppm for CB[7]·11 and 8.96 ppm for Me<sub>2</sub>CB[7]·11 (Supporting Information). We used a <sup>1</sup>H NMR competition experiment (Supporting Information) to determine that the K<sub>a</sub> value for Me<sub>2</sub>CB[7]·11 is  $3.2 \times 10^{12} \text{ M}^{-1}$ , relative to the known K<sub>a</sub> value for CB[7]·11 ( $1.98 \times 10^{12} \text{ M}^{-1}$ ).<sup>7</sup> Accordingly, it seems reasonable to expect that CB[7] derivatives like Me<sub>2</sub>CB[7] will function well as CB[7] surrogates in more complicated systems.

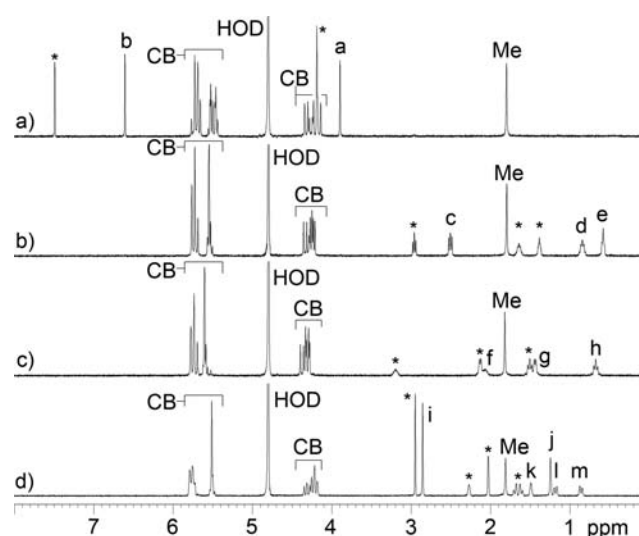


**Figure 2.** <sup>1</sup>H NMR spectra (400 MHz, D<sub>2</sub>O, room temperature) recorded for mixtures of (a) Me<sub>2</sub>CB[7] and 3 (2 equiv), (b) Me<sub>2</sub>CB[7] and 4 (2 equiv), (c) Me<sub>2</sub>CB[7] and 7 (2 equiv), and (d) Me<sub>2</sub>CB[7] and 10 (2 equiv). Resonances marked with \* arise from free guest.

**Stability of Me<sub>2</sub>CB[7].** Experiments performed by Day and co-workers established that CB[5], CB[6], and CB[7] are quite stable under the hot acidic conditions (conc HCl, 100 °C, 24 h) used in their formation.<sup>5</sup> Accordingly, we wondered whether the Me substituents on the convex face of Me<sub>2</sub>CB[7] might stabilize cationic intermediates accessible under acidic conditions and thereby accelerate decomposition reactions of Me<sub>2</sub>CB[7]. Figure 3 shows a plot of the mole fraction of Me<sub>2</sub>CB[7] versus time for a solution of Me<sub>2</sub>CB[7] heated at

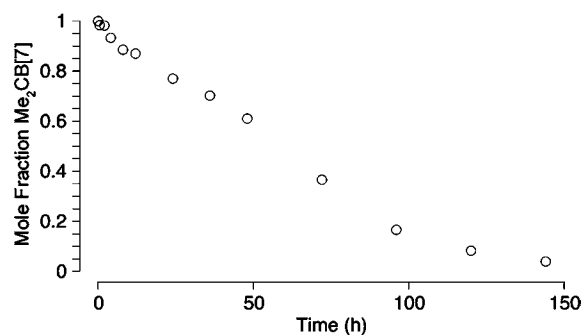


**Figure 3.** Plot of the mole fraction of Me<sub>2</sub>CB[7] upon heating at 110 °C in 9 M H<sub>2</sub>SO<sub>4</sub> as a function of time.



110 °C in 9 M H<sub>2</sub>SO<sub>4</sub>. Over the course of 6 days, Me<sub>2</sub>CB[7] completely decomposes. The <sup>1</sup>H NMR spectrum of the crude reaction mixture using **3** as probe after 6 days shows the presence of macrocycles with CB[6]-sized cavities (~24% of the crude mixture). Electrospray mass spectrometry of the crude reaction mixture allows us to identify the presence of comparable amounts of CB[6] and Me<sub>2</sub>CB[6]. Given that few applications require such highly acidic and high-temperature conditions, we believe that dialkylated CB[7] derivatives will be sufficiently stable in most situations.

**Drug Solubilization Using Me<sub>2</sub>CB[7].** One of the emerging areas for application of CB[*n*] molecular containers involves their use as solubilizing excipients for insoluble pharmaceutical agents.<sup>11,34</sup> Given the high solubility of Me<sub>2</sub>CB[7] in water, we decided to test its ability to solubilize albendazole and camptothecin, which have previously been solubilized by unsubstituted CB[7].<sup>35</sup> Figure 4 shows the phase

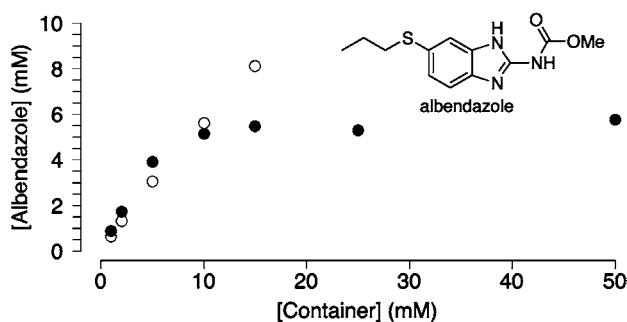


**Figure 4.** Phase solubility diagram constructed (D<sub>2</sub>O, DCl, pH 2.0, room temperature) for the solubilization of albendazole in the presence of CB[7] (○) or Me<sub>2</sub>CB[7] (●).

solubility diagrams constructed for albendazole with either Me<sub>2</sub>CB[7] or CB[7]. To construct the phase solubility diagrams,<sup>36</sup> we stirred a solution of a known concentration of host with an excess of insoluble drug overnight, filtered the solution to remove excess insoluble drug, and measured the concentration of soluble drug by <sup>1</sup>H NMR using CH<sub>3</sub>SO<sub>3</sub><sup>-</sup> as a nonbinding internal standard of known concentration. The phase solubility diagrams for albendazole and Me<sub>2</sub>CB[7] or CB[7] are quite similar at low concentrations of container (up to 10 mM). This result can be explained by the fact that the linear region of phase solubility diagrams for 1:1 host:guest complexes obeys eq 1, where *K<sub>a</sub>* is the host-guest binding

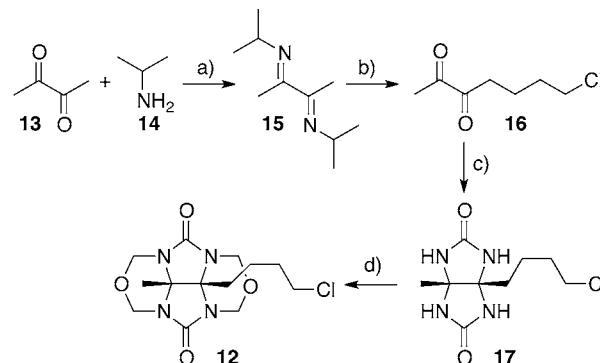
$$K_a = \frac{\text{slope}}{s_0(1 - \text{slope})} \quad (1)$$

constant (M<sup>-1</sup>) and *s*<sub>0</sub> is the intrinsic solubility of guest (drug). Given that *s*<sub>0</sub> for albendazole is the same regardless of which host is used and that the *K<sub>a</sub>* values for the CB[7]·albendazole and Me<sub>2</sub>CB[7]·albendazole are expected to be very similar, then the initial slopes should also be very similar, according to eq 1. Somewhat surprisingly, at higher concentrations of Me<sub>2</sub>CB[7] (e.g., 25–50 mM), the concentration of albendazole in solution reaches a plateau of 5.8 mM, which is lower than that achieved with 15 mM CB[7] (8.1 mM). The plateau in the phase solubility diagram for Me<sub>2</sub>CB[7]·albendazole indicates that the complex possesses only moderate solubility in water (~5.8 mM). Why does Me<sub>2</sub>CB[7]—which is far more water-soluble CB[7]—perform less well in the solubilization of

albendazole? We believe that the introduction of the Me groups on the convex face of uncomplexed Me<sub>2</sub>CB[7] dramatically increases its solubility relative to that of CB[7] because they prevent the CH...O interactions between the methine C–H groups on the convex face of one container with the ureidyl C=O portals of another container in the solid state, which has been implicated as a controlling factor in the solubility trends of CB[*n*] compounds.<sup>37</sup> Within the Me<sub>2</sub>CB[7]·albendazole and CB[7]·albendazole complexes, the drug fills the cavity and protrudes through the ureidyl C=O portals. Accordingly, the Me groups cannot enhance the solubility of Me<sub>2</sub>CB[7]·albendazole in the same way as they do Me<sub>2</sub>CB[7]. On the contrary, the presence of the hydrophobic Me groups decreases the solubility of Me<sub>2</sub>CB[7]·albendazole relative to that of CB[7]·albendazole. A similar trend was noted for the solubilization of camptothecin by CB[7] and Me<sub>2</sub>CB[7] (Supporting Information). These results suggest that a major consideration in the design of CB[*n*] derivatives for use as solubilizing excipients is the incorporation of groups designed to enhance the solubility of both the container and its container-drug complexes.

**Synthesis of Glycoluril Derivative 12.** The preparation of glycoluril derivative **12**<sup>30</sup> bearing a primary alkyl chloride is shown in Scheme 2. First, we reacted butanedione **13** with

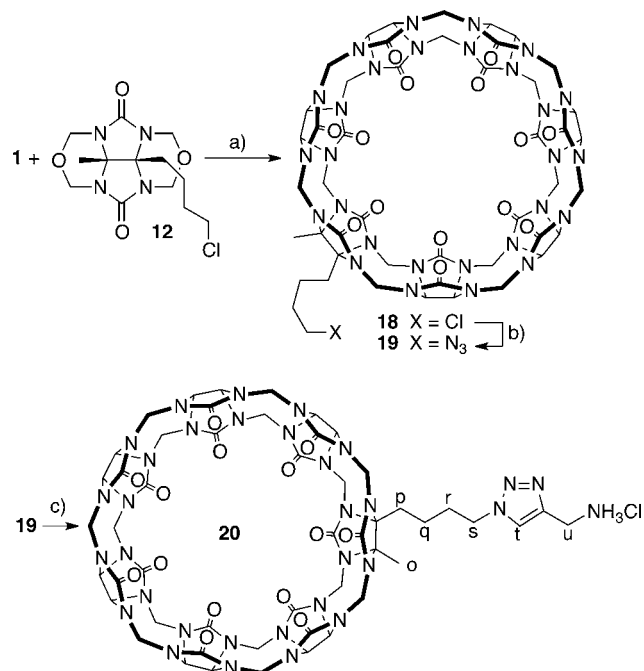
**Scheme 2.** Synthesis of Glycoluril Derivative **12**<sup>a</sup>



<sup>a</sup>Conditions: (a) Et<sub>2</sub>O, TiCl<sub>4</sub>; (b) LDA, THF, Cl(CH<sub>2</sub>)<sub>3</sub>I, 69%; (c) HCl, urea, 35%; (d) HCl, formalin, 68%.

isopropylamine **14** in Et<sub>2</sub>O with TiCl<sub>4</sub> to deliver the known diimine **15**.<sup>38</sup> Next, we deprotonated **15** with LDA in THF, followed by alkylation with 3-iodo-1-chloropropane to give **16** in 69% yield after hydrolytic workup.<sup>39</sup> Compound **16** was transformed into glycoluril **17** by reaction with urea in HCl at room temperature in 35% yield. Finally, treatment of **17** with formalin in HCl gave **12** in 68% yield.

**Synthesis of Monofunctionalized CB[7] Derivatives 18–20.** With access to gram-scale quantities of **12**, we decided to synthesize monofunctionalized CB[7] derivative **18** (Scheme 3). The reaction between **1** and **12** was conducted in 9 M H<sub>2</sub>SO<sub>4</sub> at 110 °C in the presence of KI, as developed for the synthesis of Me<sub>2</sub>CB[7], CyCB[7], and MePhCB[7] described above. The <sup>1</sup>H NMR spectrum of the crude reaction mixture obtained using **3** as probe allowed us to estimate that **18** comprised 66% of the crude material. Purification by Dowex ion-exchange chromatography allowed us to isolate 210 mg of **18** in pure form in 16% yield. Clearly, the purification process is far from ideal, and we are working to improve the process. We found that **18** can be transformed into monofunctionalized

Scheme 3. Synthesis of CB[7] Derivatives 18–20<sup>a</sup>

<sup>a</sup>Conditions: (a) 9 M H<sub>2</sub>SO<sub>4</sub>, KI, 110 °C, 16%; (b) NaN<sub>3</sub>, 80 °C, 81%; (c) 21, Pericàs's catalyst, H<sub>2</sub>O, 50 °C, 95%.

CB[7] derivative 19, which contains a reactive azide functional group, in 81% yield by simply heating with NaN<sub>3</sub> in H<sub>2</sub>O at 80 °C for 2 days. Azide 19 reacts with propargyl ammonium chloride (21) in the presence of Pericàs's catalyst<sup>40</sup> in H<sub>2</sub>O at 50 °C to give 20 in 95% yield. The <sup>1</sup>H NMR spectrum of the purified sample of 20 in the presence of 3—which is a strong binder for CB[7]-sized cavities<sup>7</sup> and thereby disrupts any potential self-assembly processes of 20—is shown in Figure 5a.

**Self-Assembly of 20 To Yield Cyclic Tetramer 20<sub>4</sub>.** We anticipated that 20, which contains both a CB[7]-sized cavity and a covalently attached triazolyl ammonium ion—which is a good guest for CB[7]-sized cavities—would undergo self-assembly processes in water. *A priori* it was hard to predict whether supramolecular polymerization processes or formation

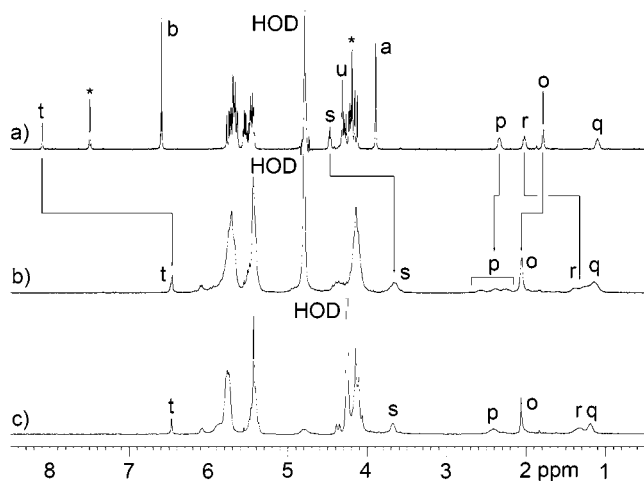


**Figure 5.** <sup>1</sup>H NMR spectra (400 MHz, D<sub>2</sub>O) recorded for mixtures of (a) 20 and 3 (1.4 equiv), (b) 20 (3.3 mM) at 20 °C, and (c) 20 (3.3 mM) at 80 °C. Resonances marked with \* arise from free 3.

of discrete cyclic assemblies would predominate.<sup>41</sup> Figure 5b shows the <sup>1</sup>H NMR spectrum recorded for a 3.3 mM solution of 20 in D<sub>2</sub>O at room temperature. A single, relatively sharp triazole C–H resonance is observed at 6.45 ppm, which suggests the formation of a well-defined assembly. On the other hand, the upfield region of the spectrum between 2.70 and 1.00 ppm, corresponding to the (CH<sub>2</sub>)<sub>4</sub> linker between the CB[7] moiety and the triazole binding unit, is broadened, and the presence of several groups of resonances suggests the presence of several different assemblies. Figure 5c shows the <sup>1</sup>H NMR spectrum recorded at 80 °C, which shows that these different groups of resonances coalesce and sharpen into four distinct resonances corresponding to each of the four CH<sub>2</sub> groups of the linking chain. The fact that the resonances for H<sub>t</sub> and H<sub>s</sub> are still strongly upfield shifted in the <sup>1</sup>H NMR spectrum recorded at 80 °C (spectrum b versus c, Figure 5) suggests that the assembly 20<sub>n</sub> persists at high temperature. To gain insight into the degree of oligomerization (*n*) of the self-assembled species (20<sub>n</sub>) formed in D<sub>2</sub>O, we performed diffusion-ordered spectroscopy (DOSY)<sup>42</sup> for the monomeric complex 20·3 and for the self-assembled species 20<sub>n</sub>, as shown in Figure 6. The diffusion coefficients measured using four different resonances for 20·3 and 20<sub>n</sub> averaged  $(2.646 \pm 0.026) \times 10^{-10}$  and  $(1.638 \pm 0.045) \times 10^{-10}$  m<sup>2</sup> s<sup>-1</sup>, respectively (Figure 6). The ratio of diffusion constants for 20·3 and 20<sub>n</sub> is 1.616. The Stokes–Einstein equation (eq 2) shows the relationship

$$D = k_B T / 6\pi\eta r_s \quad (2)$$

between the diffusion coefficient (*D*) and the hydrodynamic radius (*r<sub>s</sub>*) in a medium of viscosity *η*, where *k<sub>B</sub>* is Boltzmann's constant and *T* is temperature.<sup>42</sup> If we assume that 20·3 and 20<sub>n</sub> are roughly spherical, then the ratio of the measured diffusion coefficients can be converted into a ratio of molecular weights, which gives the oligomerization number. For trimeric, tetrameric, and pentameric assemblies, theory predicts the ratios *D*(20·3)/*D*(20<sub>n</sub>) = 1.442 (*n* = 3), 1.587 (*n* = 4), and 1.709 (*n* = 5). In this manner, the measured ratio of diffusion coefficients of 1.616 strongly suggests the formation of the cyclic tetrameric assembly 20<sub>4</sub>.

To provide additional evidence for the formation of the cyclic tetrameric assembly 20<sub>4</sub>, we performed electrospray ionization mass spectrometry of 100 μM solutions in H<sub>2</sub>O and 100 000 resolution on an LTQ-Orbitrap instrument (Thermo-Fisher, San Jose, CA). Figure 7a shows the mass spectrum obtained, which incitates a 4+ ion at *m/z* = 1329.97, a 5+ ion at *m/z* = 1068.68, and a 6+ ion at *m/z* = 894.31. The 4+ ion corresponds to the 20<sub>4</sub><sup>4+</sup> assembly. Figure 7b shows the expansion of the region of the 20<sub>4</sub><sup>4+</sup> ion, and Figure 7c shows the theoretical ion distribution for molecular formula C<sub>200</sub>H<sub>228</sub>N<sub>128</sub>O<sub>56</sub>. The excellent match between panels b and c in Figure 7 provides strong evidence for the description of this structure as the cyclic tetramer 20<sub>4</sub><sup>4+</sup>. Other ions of significant intensity in Figure 7a were observed at *m/z* = 1068.68, which corresponds to [20<sub>4</sub>·Na]<sup>5+</sup>, and *m/z* = 894.31, which corresponds to [20<sub>4</sub>·Na<sub>2</sub>]<sup>6+</sup>. To gain further insight into this system, we isolated ion 20<sub>4</sub><sup>4+</sup> and performed collision-induced dissociation experiments (Figure 7d). We observed the cleavage of covalent bonds rather than the expected dissociation of non-covalent aggregate 20<sub>4</sub><sup>4+</sup> into smaller non-covalent aggregate ions (e.g., monomers, dimers, or trimers). Overall, the electrospray mass spectrometric

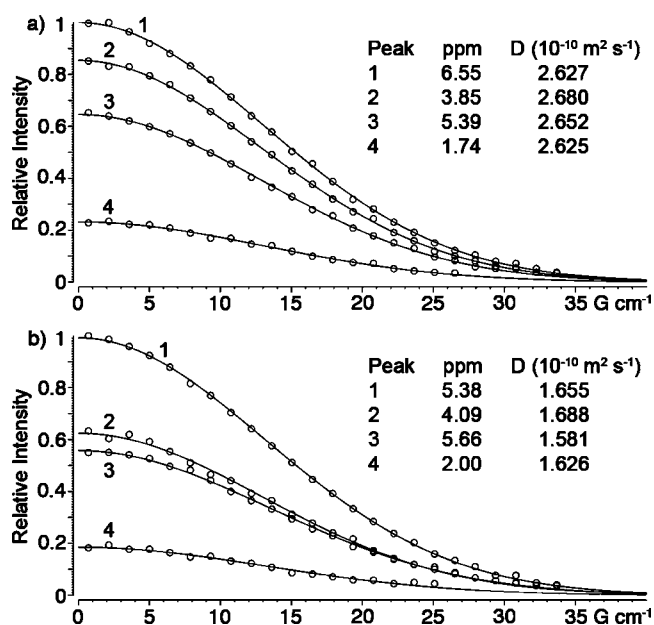


Figure 6. DOSY spectra recorded (600 MHz, D<sub>2</sub>O, room temperature) for (a) 20·3 and (b) cyclic tetramer 20<sub>4</sub>.

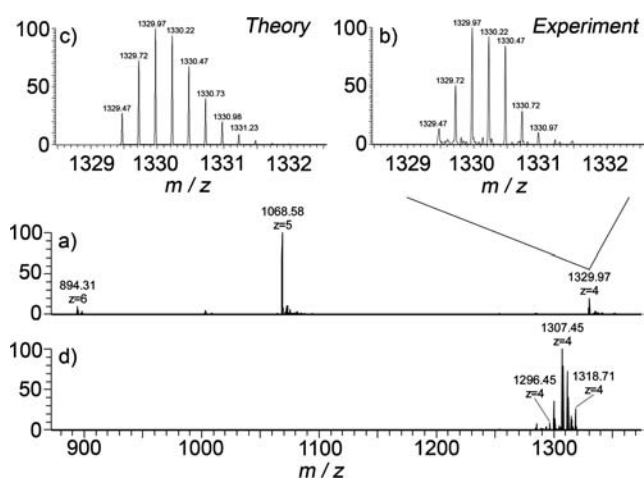
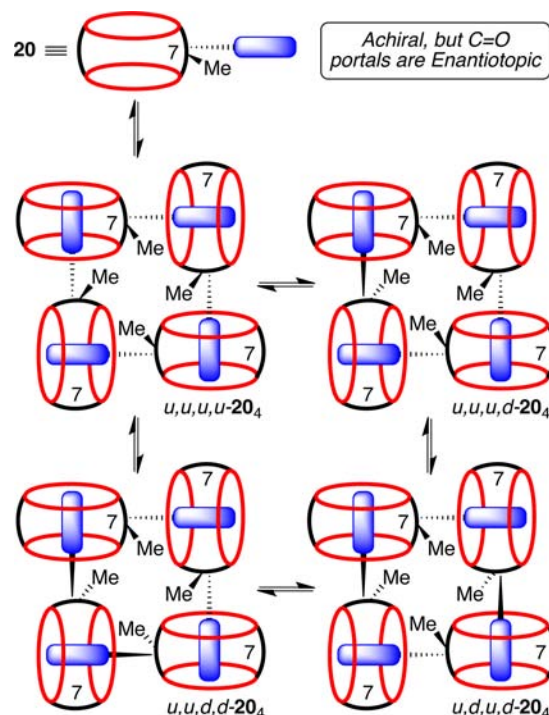


Figure 7. Electrospray ionization mass spectra recorded for (a) a solution of 1<sub>4</sub> (100 μM, H<sub>2</sub>O), (b) expansion of the 1<sub>4</sub><sup>4+</sup> ion region, and (c) theoretical distribution obtained for the molecular formula C<sub>200</sub>H<sub>228</sub>N<sub>128</sub>O<sub>56</sub><sup>4+</sup>. (d) Mass spectrum obtained upon collision-induced dissociation.

investigations strongly support that 20 self-assembles to give a highly stable cyclic tetrameric aggregate 20<sub>4</sub><sup>4+</sup>.

**Enumeration of the Different Diastereomers of 20<sub>4</sub>.** Although compound 1 is achiral due to the presence of a mirror plane that runs through the equator of the molecule, complexation events that desymmetrize the cavity result in the formation of complexes that are enantiomers, and the two C=O portals can be described as enantiotopic. Accordingly, when four molecules of 1 self-assemble to form 1<sub>4</sub>, there are several diastereomers that can form (Scheme 4). For example, all four Me groups can be pointing up (u,u,u,u-1<sub>4</sub>), three up and one down (u,u,u,d-1<sub>4</sub>), and two different combinations of two up and two down (u,u,d,d-1<sub>4</sub> and u,d,u,d-1<sub>4</sub>).<sup>43</sup> The various diastereomers are able to interconvert with one another by a sequence of dissociation of one of the CB[7]·triazolyl ammonium complexes to give a linear tetramer, followed by

Scheme 4. Self-Assembly of CB[7] Derivative 20 To Give the Cyclic Tetramer 20<sub>4</sub> as a Mixture of Diastereomers



rotation of the CB[7] group and re-complexation of the triazolyl ammonium through the opposite ureidyl C=O portal of the CB[7] moiety. In this way, averaging of the signals observed in the high-temperature <sup>1</sup>H NMR spectrum shown in Figure 5c is readily understandable.

## CONCLUSION

In summary, we have shown that CB[7] derivatives are accessible by a building-block approach that involves the condensation of glycoluril hexamer 1 with glycoluril bis(cyclic ethers) 2<sub>Me</sub>, 2<sub>Cy</sub>, 2<sub>MePh</sub>, and 12. Just like CB[7] itself, the high water solubility of Me<sub>2</sub>CB[7] and its outstanding host-guest recognition properties make it well suited as a solubilization agent for poorly soluble pharmaceutical agents. Compound 18, which bears a reactive primary alkyl chloride group, is the first monofunctionalized CB[7] derivative to be reported. Compound 18 undergoes further functionalization reactions to yield 19 and subsequently 20 by click chemistry. We find that 20 undergoes a self-assembly process in water to yield cyclic tetramer 1<sub>4</sub> as established by NMR (VT and DOSY) and mass spectrometric measurements.

We believe that the implications of this research go well beyond the system-specific details described above. For example, unfunctionalized CB[7] has been the most widely applied CB[n] compound because of its good solubility in water and its exceptional binding affinity and selectivity toward its guests in water. This paper provides two water-soluble monofunctionalized CB[7] derivatives that are amenable to further functionalization reactions by S<sub>N</sub>2 and click chemistry, which promises to allow the homogeneous covalent attachment of CB[7] to solid phases—macromolecules like proteins and polymers—and incorporation into other complex and functional (bio)molecular systems. When that occurs, the continued impact of the CB[n] family of molecular containers on the chemical sciences will be significant.



## EXPERIMENTAL SECTION

**Compound 18.** A mixture of **1** (1.00 g, 1.03 mmol) and KI (0.230 g, 1.35 mmol) was dissolved in 9 M aqueous H<sub>2</sub>SO<sub>4</sub> (5 mL) and then treated with **12** (0.510 g, 1.55 mmol). The flask was then sealed with a rubber septum and heated at 110 °C for 30 min. The reaction solution was poured into MeOH (40 mL), which resulted in a gray precipitate. The mixture was centrifuged at 7200 rpm for 5 min. The supernatant was decanted, and the precipitate was washed with MeOH (40 mL × 3) and centrifuged at 7200 rpm for 5 min. The precipitate was dried under high vacuum to give a crude, gray powder (1.46 g). The crude solid was dissolved in 88% formic acid/0.4 M HCl (1:1, v:v, 10 mL). The solution containing the crude solid was loaded onto a column (3 cm diameter × 20 cm long) containing Dowex 50WX2 ion-exchange resin pretreated with 88% formic acid/0.4 M HCl (1:1, v:v). The column was eluted with 88% formic acid/0.4 M HCl (1:1, v:v, 400 mL), and then 88% formic acid/0.6 M HCl (1:1, v:v, 400 mL), and then 88% formic acid/0.8 M HCl (1:1, v:v, 400 mL). The fraction purity was assessed by <sup>1</sup>H NMR using **3** as a probe. The appropriate fractions were combined, solvent was removed by rotary evaporation, and the precipitate was dried under high vacuum. The yellow solid was then washed with MeOH (40 mL) and centrifuged at 7200 rpm for 5 min. The supernatant was decanted, and the precipitate was dried under high vacuum to give **18** as a white powder (0.21 g, 0.16 mmol, 16%). Mp: >300 °C. IR (KBr, cm<sup>-1</sup>): 3001w, 2917w, 1729s, 1479s, 1423m, 1376m, 1321s, 1290m, 1235s, 1193s, 968m, 828m, 807s. <sup>1</sup>H NMR (500 MHz, D<sub>2</sub>O, >1 equiv of **3**): 7.51 (s, unbound **3**), 6.62 (s, 4H), 5.80–5.65 (m, 14H), 5.60–5.40 (m, 12H), 4.40–4.20 (m, 10H), 4.21 (s, unbound **3**), 4.16 (d, J = 15.4, 4H), 3.92 (s, 4H), 3.64 (t, J = 6.3, 2H), 2.40–2.30 (m, 2H), 1.90 (s, 3H), 1.95–1.85 (m, 2H), 1.40–1.30 (m, 2H). <sup>13</sup>C NMR (125 MHz, D<sub>2</sub>O, dioxane as internal reference, >1 equiv of **3**): 156.8, 156.7, 156.5, 156.5, 156.5, 156.2, 133.7, 133.6, 129.6, 128.0, 80.5, 78.8, 71.7, 71.6, 71.5, 71.4, 71.3, 71.2, 71.2, 71.1, 70.3, 53.2, 53.1, 52.6, 52.6, 52.3, 49.3, 48.9, 44.8, 42.7, 42.4, 31.2, 27.4, 19.6, 14.7 (only 35 of the 39 resonances expected were observed). HR-MS: *m/z* 702.2476 ([**18-3**]<sup>2+</sup>, calcd for C<sub>47</sub>H<sub>51</sub>ClN<sub>28</sub>O<sub>14</sub>·C<sub>8</sub>H<sub>14</sub>N<sub>2</sub><sup>2+</sup>, 702.2493).

**Compound 19.** A mixture of **18** (100 mg, 0.079 mmol) and NaN<sub>3</sub> (39 mg, 0.60 mmol) was dissolved in H<sub>2</sub>O (2 mL). The mixture was heated at 80 °C for 2 days. The reaction solution was poured into MeOH (3 mL), which resulted in a gray precipitate. The mixture was centrifuged at 7200 rpm for 5 min. The supernatant was decanted, and the precipitate was washed with MeOH (5 mL × 3) and centrifuged at 7200 rpm for 5 min. The precipitate was dried under high vacuum to give **19** as a white powder (81 mg, 0.064 mmol, 81%). Mp: >300 °C. IR (KBr, cm<sup>-1</sup>): 3442m, 3001w, 2923w, 2099w, 2034m, 1729s, 1476s, 1420m, 1378m, 1322m, 1236s, 1192m, 971m. <sup>1</sup>H NMR (400 MHz, D<sub>2</sub>O, >1 equiv of **3**): 7.47 (s, unbound **3**), 6.62 (s, 4H), 5.80–5.60 (m, 14H), 5.60–5.40 (m, 12H), 4.35 (d, J = 16.0, 2H), 4.29 (d, J = 15.6, 4H), 4.23 (d, J = 15.6, 2H), 4.22 (d, J = 15.6, 2H), 4.15 (d, J = 15.6, 4H), 4.13 (s, unbound **3**), 3.91 (s, 4H), 3.36 (t, J = 6.2, 2H), 2.40–2.30 (m, 2H), 1.89 (s, 3H), 1.75–1.65 (m, 2H), 1.35–1.25 (m, 2H). <sup>13</sup>C NMR (125 MHz, D<sub>2</sub>O, dioxane as internal reference, >1 equiv of **3**): 156.7, 156.6, 156.5, 156.5, 156.4, 156.2, 134.3, 134.3, 128.3, 127.8, 80.4, 78.8, 71.7, 71.6, 71.6, 71.5, 71.4, 71.3, 71.2, 71.2, 71.0, 70.3, 53.1, 53.0, 52.6, 52.5, 52.3, 50.6, 49.2, 48.8, 43.9, 42.6, 27.6, 19.6, 14.7 (only 35 of the 39 resonances expected were observed). HR-MS: *m/z* 705.7703 ([**19-3**]<sup>2+</sup>, calcd for C<sub>47</sub>H<sub>51</sub>N<sub>31</sub>O<sub>14</sub>·C<sub>8</sub>H<sub>14</sub>N<sub>2</sub><sup>2+</sup>, 705.7694).

**Compound 20.** A mixture of **19** (50 mg, 0.039 mmol), propargyl amine hydrochloride (**21**, 36 mg, 0.39 mmol), and Pericàs' catalyst (0.0039 mmol, 2.4 mg)<sup>40</sup> was dissolved in H<sub>2</sub>O (2 mL). The mixture was heated at 50 °C for 1 day. The reaction solution was poured into MeOH (3 mL), which resulted in a gray precipitate. The mixture was centrifuged at 7200 rpm for 5 min. The supernatant was decanted, and the precipitate was washed with MeOH (5 mL × 3) and centrifuged at 7200 rpm for 5 min. The precipitate was dried under high vacuum to give **20** as a white powder (50 mg, 0.037 mmol, 95%). Mp: >300 °C. IR (KBr, cm<sup>-1</sup>): 3442m, 2994w, 2916w, 1729s, 1473s, 1422m, 1378m, 1322m, 1235s, 1194m, 970m. <sup>1</sup>H NMR (500 MHz, D<sub>2</sub>O, >1 equiv of **3**): 8.10 (s, 1H), 7.50 (s, unbound **3**), 6.61 (s, 4H), 5.80–5.60 (m,

14H), 5.60–5.40 (m, 12H), 4.48 (t, J = 6.3, 2H), 4.32 (s, 2H), 4.35–4.20 (m, 10H), 4.20 (s, unbound **3**), 4.15 (d, J = 15.4, 4H), 3.89 (s, 4H), 2.40–2.30 (m, 2H), 2.10–2.00 (m, 2H), 1.79 (s, 3H), 1.15–1.05 (m, 2H). <sup>13</sup>C NMR (125 MHz, D<sub>2</sub>O, dioxane as internal reference, >1 equiv of **3**): 156.7, 156.7, 156.5, 156.5, 156.5, 156.1, 133.7, 133.6, 129.6, 128.0, 125.4, 80.4, 78.7, 71.7, 71.6, 71.5, 71.4, 71.3, 71.2, 71.2, 71.1, 53.2, 53.1, 52.6, 52.6, 52.3, 49.9, 49.2, 48.8, 42.7, 42.4, 34.0, 28.8, 27.4, 19.1, 14.7 (only 36 of the 42 resonances expected were observed). HR-MS: *m/z* 733.2910 ([**20-3**]<sup>2+</sup>, calcd for C<sub>50</sub>H<sub>56</sub>N<sub>32</sub>O<sub>14</sub>·C<sub>8</sub>H<sub>14</sub>N<sub>2</sub><sup>2+</sup>, 733.2905).

## ASSOCIATED CONTENT

### Supporting Information

Synthetic procedures; characterization data and <sup>1</sup>H and <sup>13</sup>C NMR spectra for all new compounds; <sup>1</sup>H NMR spectra for host–guest complexes; details of the X-ray structure of Me<sub>2</sub>CB[7]·**3**; <sup>1</sup>H NMR spectra used for *K<sub>rel</sub>* calculation; ES-MS data for the decomposition reaction of Me<sub>2</sub>CB[7]; and MMFF-minimized models of **20**. This material is available free of charge via Internet at <http://pubs.acs.org>.

## AUTHOR INFORMATION

### Corresponding Author

LIsaacs@umd.edu

### Author Contributions

<sup>‡</sup>B.V. and L.C. contributed equally.

### Notes

The authors declare no competing financial interest.

## ACKNOWLEDGMENTS

We thank Dr. Derick Lucas for initial experiments directed toward the preparation of Me<sub>2</sub>CB[7]. We thank the National Science Foundation (CHE-1110911 to L.I.) and the National Institutes of Health (GM021248 to C.F.) for financial support. This paper is dedicated to Prof. François Diederich on the occasion of his 60th birthday.

## REFERENCES

- (1) Lee, J. W.; Samal, S.; Selvapalam, N.; Kim, H.-J.; Kim, K. *Acc. Chem. Res.* **2003**, *36*, 621–630.
- (2) Lagona, J.; Mukhopadhyay, P.; Chakrabarti, S.; Isaacs, L. *Angew. Chem., Int. Ed.* **2005**, *44*, 4844–4870. Nau, W. M.; Florea, M.; Assaf, K. *I. Isr. J. Chem.* **2011**, *51*, 559–577. Masson, E.; Ling, X.; Joseph, R.; Kyeremeh-Mensah, L.; Lu, X. *RSC Adv.* **2012**, *2*, 1213–1247.
- (3) Freeman, W. A.; Mock, W. L.; Shih, N.-Y. *J. Am. Chem. Soc.* **1981**, *103*, 7367–7368. Day, A. I.; Blanch, R. J.; Arnold, A. P.; Lorenzo, S.; Lewis, G. R.; Dance, I. *Angew. Chem., Int. Ed.* **2002**, *41*, 275–277. Liu, S.; Zavalij, P. Y.; Isaacs, L. *J. Am. Chem. Soc.* **2005**, *127*, 16798–16799.
- (4) Kim, J.; Jung, I.-S.; Kim, S.-Y.; Lee, E.; Kang, J.-K.; Sakamoto, S.; Yamaguchi, K.; Kim, K. *J. Am. Chem. Soc.* **2000**, *122*, 540–541.
- (5) Day, A. I.; Arnold, A. P.; Blanch, R. J.; Snushall, B. J. *Org. Chem.* **2001**, *66*, 8094–8100.
- (6) Mock, W. L.; Shih, N. Y. *J. Org. Chem.* **1986**, *51*, 4440–4446.
- (7) Liu, S.; Ruspic, C.; Mukhopadhyay, P.; Chakrabarti, S.; Zavalij, P. Y.; Isaacs, L. *J. Am. Chem. Soc.* **2005**, *127*, 15959–15967.
- (8) Rekharsky, M. V.; Mori, T.; Yang, C.; Ko, Y. H.; Selvapalam, N.; Kim, H.; Sobransingh, D.; Kaifer, A. E.; Liu, S.; Isaacs, L.; Chen, W.; Moghaddam, S.; Gilson, M. K.; Kim, K.; Inoue, Y. *Proc. Natl. Acad. Sci. U.S.A.* **2007**, *104*, 20737–20742.
- (9) Uzunova, V. D.; Cullinane, C.; Brix, K.; Nau, W. M.; Day, A. I. *Org. Biomol. Chem.* **2010**, *8*, 2037–2042. McInnes, F. J.; Anthony, N. G.; Kennedy, A. R.; Wheate, N. J. *Org. Biomol. Chem.* **2010**, *8*, 765–773. Angelos, S.; Khashab, N. M.; Yang, Y.-W.; Trabolsi, A.; Khatib, H. A.; Stoddart, J. F.; Zink, J. I. *J. Am. Chem. Soc.* **2009**, *131*, 12912–12914. Zhang, J.; Coulston, R. J.; Jones, S. T.; Geng, J.; Scherman, O. A.; Abell, C. *Science* **2012**, *335*, 690–694.

- (10) Kim, E.; Kim, D.; Jung, H.; Lee, J.; Paul, S.; Selvapalam, N.; Yang, Y.; Lim, N.; Park, C. G.; Kim, K. *Angew. Chem., Int. Ed.* **2010**, *49*, 4405–4408.
- (11) Ma, D.; Hettiarachchi, G.; Nguyen, D.; Zhang, B.; Wittenberg, J. B.; Zavalij, P. Y.; Briken, V.; Isaacs, L. *Nat. Chem.* **2012**, *4*, 503–510.
- (12) Jeon, W. S.; Ziganshina, A. Y.; Lee, J. W.; Ko, Y. H.; Kang, J.-K.; Lee, C.; Kim, K. *Angew. Chem., Int. Ed.* **2003**, *42*, 4097–4100. Ko, Y. H.; Kim, E.; Hwang, I.; Kim, K. *Chem. Commun.* **2007**, 1305–1315. Jeon, W. S.; Kim, E.; Ko, Y. H.; Hwang, I.; Lee, J. W.; Kim, S.-Y.; Kim, H.-J.; Kim, K. *Angew. Chem., Int. Ed.* **2005**, *44*, 87–91.
- (13) Appel, E. A.; Biedermann, F.; Rauwald, U.; Jones, S. T.; Zayed, J. M.; Scherman, O. A. *J. Am. Chem. Soc.* **2010**, *132*, 14251–14260. Wang, W.; Kaifer, A. E. *Angew. Chem., Int. Ed.* **2006**, *45*, 7042–7046. Kim, K.; Kim, D.; Lee, J. W.; Ko, Y. H.; Kim, K. *Chem. Commun.* **2004**, 848–849. Liu, Y.; Yu, Y.; Gao, J.; Wang, Z. *Angew. Chem., Int. Ed.* **2010**, *49*, 6576–6579.
- (14) Ghale, G.; Ramalingam, V.; Urbach, A. R.; Nau, W. M. *J. Am. Chem. Soc.* **2011**, *133*, 7528–7535. Biedermann, F.; Rauwald, U.; Cziferszky, M.; Williams, K. A.; Gann, L. D.; Guo, B. Y.; Urbach, A. R.; Bielawski, C. W.; Scherman, O. A. *Chem.—Eur. J.* **2010**, *16*, 13716–13722. Baumes, L. A.; Sogo, M. B.; Montes-Navajés, P.; Corma, A.; Garcia, H. *Chem.—Eur. J.* **2010**, *16*, 4489–4495. Wu, J.; Isaacs, L. *Chem.—Eur. J.* **2009**, *15*, 11675–11680.
- (15) Liu, S.; Zavalij, P. Y.; Lam, Y.-F.; Isaacs, L. *J. Am. Chem. Soc.* **2007**, *129*, 11232–11241. Ghosh, S.; Isaacs, L. *J. Am. Chem. Soc.* **2010**, *132*, 4445–4454. Kim, C.; Agasti, S. S.; Zhu, Z.; Isaacs, L.; Rotello, V. M. *Nat. Chem.* **2010**, *2*, 962–966. Nguyen, H. D.; Dang, D. T.; van Dongen, J. L. J.; Brunsveld, L. *Angew. Chem., Int. Ed.* **2010**, *49*, 895–898. Chinai, J. M.; Taylor, A. B.; Ryno, L. M.; Hargreaves, N. D.; Morris, C. A.; Hart, P. J.; Urbach, A. R. *J. Am. Chem. Soc.* **2011**, *133*, 8810–8813.
- (16) Jon, S. Y.; Selvapalam, N.; Oh, D. H.; Kang, J.-K.; Kim, S.-Y.; Jeon, Y. J.; Lee, J. W.; Kim, K. *J. Am. Chem. Soc.* **2003**, *125*, 10186–10187.
- (17) Kim, K.; Selvapalam, N.; Ko, Y. H.; Park, K. M.; Kim, D.; Kim, J. *Chem. Soc. Rev.* **2007**, *36*, 267–279.
- (18) Lee, D.-W.; Park, K. M.; Banerjee, M.; Ha, S. H.; Lee, T.; Suh, K.; Paul, S.; Jung, H.; Kim, J.; Selvapalam, N.; Ryu, S. H.; Kim, K. *Nat. Chem.* **2011**, *3*, 154–159.
- (19) Park, K. M.; Yang, J.-A.; Jung, H.; Yeom, J.; Park, J. S.; Park, K.-H.; Hoffman, A. S.; K., H. S.; Kim, K. *ACS Nano* **2012**, *6*, 2960–2968.
- (20) Zhao, N.; Lloyd, G. O.; Scherman, O. A. *Chem. Commun.* **2012**, 48, 3070–3072.
- (21) Chakraborty, A.; Wu, A.; Witt, D.; Lagona, J.; Fettinger, J. C.; Isaacs, L. *J. Am. Chem. Soc.* **2002**, *124*, 8297–8306.
- (22) Huang, W.-H.; Zavalij, P. Y.; Isaacs, L. *J. Am. Chem. Soc.* **2008**, *130*, 8446–8454.
- (23) Ma, D.; Gargulakova, Z.; Zavalij, P. Y.; Sindelar, V.; Isaacs, L. *J. Org. Chem.* **2010**, *75*, 2934–2941.
- (24) Lucas, D.; Minami, T.; Iannuzzi, G.; Cao, L.; Wittenberg, J. B.; Anzenbacher, P. J.; Isaacs, L. *J. Am. Chem. Soc.* **2011**, *133*, 17966–17976.
- (25) Huang, W.-H.; Liu, S.; Zavalij, P. Y.; Isaacs, L. *J. Am. Chem. Soc.* **2006**, *128*, 14744–14745. Huang, W.-H.; Zavalij, P. Y.; Isaacs, L. *Angew. Chem., Int. Ed.* **2007**, *46*, 7425–7427. Hettiarachchi, G.; Nguyen, D.; Wu, J.; Lucas, D.; Ma, D.; Isaacs, L.; Briken, V. *PLoS One* **2010**, *5*, e10514. Ma, D.; Zavalij, P. Y.; Isaacs, L. *J. Org. Chem.* **2010**, *75*, 4786–4795.
- (26) Cao, L.; Isaacs, L. *Org. Lett.* **2012**, *14*, 3072–3075.
- (27) Wu, F.; Wu, L.-H.; Zhang, Y.-Q.; Xue, S.-F.; Tao, Z.; Day, A. I. *J. Org. Chem.* **2012**, *77*, 606–611.
- (28) Day, A. I.; Arnold, A. P.; Blanch, R. J. *Molecules* **2003**, *8*, 74–84. Lagona, J.; Fettinger, J. C.; Isaacs, L. *Org. Lett.* **2003**, *5*, 3745–3747. Wittenberg, J. B.; Costales, M. G.; Zavalij, P. Y.; Isaacs, L. *Chem. Commun.* **2011**, 47, 9420–9422.
- (29) Zhao, Y.; Xue, S.; Zhu, Q.; Tao, Z.; Zhang, J.; Wei, Z.; Long, L.; Hu, M.; Xiao, H.; Day, A. I. *Chin. Sci. Bull.* **2004**, *49*, 1111–1116.
- (30) Day, A. I.; Arnold, A. P.; Blanch, R. J. (Unisearch Limited). Method for Preparing Cucurbiturils. WO 2005/026168 A1, 2005.
- (31) We choose to use 9 M H<sub>2</sub>SO<sub>4</sub> because this was the solvent used in the high-yielding synthesis of CB[7] reported by Nau and to use KI because metal ions are known from the work of Day to influence the distribution of CB[n] obtained. Analysis of the crude reaction mixtures of **1** and **12** in 9 M H<sub>2</sub>SO<sub>4</sub> in the absence of KI shows that they contain less **18** (CB[6], 70%; **18**, 25%) that do reactions mixtures in concentrated HCl in the presence of KI (CB[6], 70%; **18**, 30%) or the absence of KI (CB[6], 59%; **18**, 39%), as shown in the Supporting Information. See: Marquez, C.; Huang, F.; Nau, W. M. *IEEE Trans. Nanobiosci.* **2004**, *3*, 39–45. Day, A. I.; Blanch, R. J.; Coe, A.; Arnold, A. P. *J. Inclusion Phenom. Macrocycl. Chem.* **2002**, *43*, 247–250.
- (32) Stella, V. J.; Rajewski, R. A. *Pharm. Res.* **1997**, *14*, 556–567. De Greef, T. F. A.; Smulders, M. M. J.; Wolffs, M.; Schenning, A. P. H. J.; Sijbesma, R. P.; Meijer, E. W. *Chem. Rev.* **2009**, *109*, 5687.
- (33) Witt, D.; Lagona, J.; Damkaci, F.; Fettinger, J. C.; Isaacs, L. *Org. Lett.* **2000**, *2*, 755–758. Wu, A.; Chakraborty, A.; Witt, D.; Lagona, J.; Damkaci, F.; Ofori, M. A.; Chiles, J. K.; Fettinger, J. C.; Isaacs, L. *J. Org. Chem.* **2002**, *67*, 5817–5830.
- (34) Walker, S.; Oun, R.; McInnes, F. J.; Wheate, N. J. *Isr. J. Chem.* **2011**, *51*, 616–624. Ghosh, I.; Nau, W. M. *Adv. Drug Delivery Rev.* **2012**, *64*, 764–783. Day, A. I.; Collins, J. G. *Supramol. Chem. Mol. Nanomater.* **2012**, *3*, 983–1000.
- (35) Zhao, Y.; Buck, D. P.; Morris, D. L.; Pourgholami, M. H.; Day, A. I.; Collins, J. G. *Org. Biomol. Chem.* **2008**, *6*, 4509–4515. Koner, A. L.; Ghosh, I.; Saleh, N. i.; Nau, W. M. *Can. J. Chem.* **2011**, *89*, 139–147. Dong, N.; Xue, S.-F.; Zhu, Q.-J.; Tao, Z.; Zhao, Y.; Yang, L.-X. *Supramol. Chem.* **2008**, *20*, 659–665.
- (36) Connors, K. A. *Binding Constants*; John Wiley & Sons: New York, 1987.
- (37) Bardelang, D.; Udachin, K. A.; Leek, D. M.; Margeson, J. C.; Chan, G.; Ratcliffe, C. I.; Ripmeester, J. A. *Cryst. Growth Des.* **2011**, *11*, 5598–5614.
- (38) Kimpe, N. D.; D'Hondt, L.; Stanoeva, E. *Tetrahedron Lett.* **1991**, *32*, 3879–3882.
- (39) Kimpe, N. D.; Stevens, C. *Tetrahedron* **1995**, *51*, 2387–2402.
- (40) Ozcubukcu, S.; Okzal, E.; Jimeno, C.; Pericàs, M. *Org. Lett.* **2009**, *11*, 6480–6483.
- (41) Park, K.-M.; Kim, S.-Y.; Heo, J.; Whang, D.; Sakamoto, S.; Yamaguchi, K.; Kim, K. *J. Am. Chem. Soc.* **2002**, *124*, 2140–2147. Ko, Y. H.; Kim, K.; Kang, J.-K.; Chun, H.; Lee, J. W.; Sakamoto, S.; Yamaguchi, K.; Fettinger, J. C.; Kim, K. *J. Am. Chem. Soc.* **2004**, *126*, 1932–1933. Da Silva, J. P.; Jayaraj, N.; Jockusch, S.; Turro, N.; Ramamurthy, V. *Org. Lett.* **2011**, *13*, 2410–2413.
- (42) Cohen, Y.; Avram, L.; Frisch, L. *Angew. Chem., Int. Ed.* **2005**, *44*, 520–554.
- (43) Assemblies u,u,u,u-**14** and u,u,u,d-**14** are chiral with enantiomers d,d,d,d-**14** and d,d,d,u-**14**. Assemblies u,u,d,d-**14** and u,d,u,d-**14** are achiral due the presence of an inversion center and an S<sub>4</sub>-axis, respectively.